IF-Free Sub-6GHz and mmW Band Integrated RoF Fronthaul Using Low-Pass Delta-Sigma Modulator and RZ Shaping

Yixiao Zhu(1), Xiansong Fang(2), Chenbo Zhang(2), Yicheng Xu(1), Qunbi Zhuge(1), Xiaopeng Xie(2), Fan Zhang(2), and Weisheng Hu(1)

(1) State Key Laboratory of Advanced Optical Communication System and Networks, Shanghai Jiao Tong University, Shanghai, 200240, China, yixiaozhu@sjtu.edu.cn
(2) State Key Laboratory of Advanced Optical Communication System and Networks, Peking University, Beijing, 100871, China

Abstract *We propose a low-complexity and IF-free radio-over-fiber scheme using low-pass delta-sigma modulator and RZ shaping for both sub-6GHz and millimeter-wave bands. Up to 262144-QAM, 65536-QAM and 4096-QAM formats are experimentally delivered at 28-GHz, 30-GHz, and 48-GHz carrier frequency over a 10-km IM-DD SMF link, respectively.*

Introduction

The emerging bandwidth-consuming services in 5G Era are putting higher requirements on the cloud radio access network (C-RAN) in terms of bandwidth, fidelity, and coverage [1]. To extend the congested wireless spectrum, 5G new radio (NR) has standardized both Sub-6GHz and millimeter-wave (mmW) bands above 24 GHz [2]. As the cell area reduces, simplifying the structure of radio units (RUs) becomes particularly crucial for massive dense and seamless access.

In general, the transmission of a wireless waveform in fronthaul link mainly relies on digital or analog radio-over-fiber (D-/A-RoF) techniques [3-7]. Recently, delta-sigma modulation (DSM) has been considered a promising solution for point-to-multipoint (PTMP) architecture [8]. It digitizes the original wireless waveform after over-sampling and noise shaping, and recover it through an analog band-pass filter [9]. In Ref. [10], carrier aggregation of 32×4G-LTE or 30×5G-FBMC signals is experimentally demonstrated in a 10-Gb/s intensity modulation with direct detection (IM-DD) link. Based on 200-G coherent transceiver, 20×192-MHz DOCSIS3.1 channels with 16384-QAM can be supported [11].

However, moving to higher-frequency mmW band, the high over-sampling rate of DSM becomes a critical problem. In Ref. [12], by interleaving the in-phase (I) and quadrature (Q) outputs of low-pass DSM into patterns of {I, Q, -I, -Q}, real-time implementation of 100-GSa/s DSM is reported for the 22.75-27.5-GHz band, where the carrier frequency (IF) is only 1/4 of the sampling rate ($\mathrm{F_s}$). Alternatively, with Manchester coding as {-I, I}, the required sampling rate can be reduced to twice of the carrier frequency [13]. The drawback is the halved transmission bandwidth due to coding redundancy. Moreover, the application of high-pass DSM [14] achieves the lowest sampling rate of $2{\cdot}\mathrm{IF}$ and maximum bandwidth of $2{\cdot}\mathrm{IF/OSR}$, but requiring additional efforts on DSM coefficients optimization and up-conversion of the input wireless waveform.

In this work, we propose and experimentally demonstrate an IF-free RoF scheme based on low-pass DSM and return-to-zero (RZ) shaping. The signal replica is directly mapped to both the baseband and high-frequency band around $F_s/2$ without up-conversion after zero insertion. The coding redundancy can be fully avoided by interleaving two data streams in the time domain. Both low- and high-pass filters are feasible for wireless signal recovery, thus it is compatible with Sub-6GHz and mmW band applications. Based on 2-bit, 1.5-bit, and 1-bit low-pass DSM, we successfully deliver up to 262144-QAM, 65536-QAM, and 4096-QAM at 28 GHz, 30 GHz, and 48 GHz carrier frequency over a 10-km IM-DD link.

Principle

Fig. 1 illustrates the principle of the proposed IF-free scheme based on RZ shaping. At the transmitter side, a low-pass DSM transforms two independent baseband wireless waveforms into digitized sample sequences A and B, respectively. The quantization noise is pushed out of the signal band below the Nyquist frequency of $\mathrm{OSR}{\cdot}\mathrm{F_s}/2$. Here OSR represents the over-sampling rate, and $\mathrm{F_s}$ is the sampling rate of the low-pass DSM. Then the output sequence is 2-time up-sampled, where zeros are added on the even (or odd) time slots for sequence A (or B). As a result, the Nyuiqst region is extended to [-$\mathrm{OSR}{\cdot}\mathrm{F_s}$, $\mathrm{OSR}{\cdot}\mathrm{F_s}$]. According to the property of RZ pulse, two signal replicas appear at the baseband and high-frequency bands of $\mathrm{IF}=\mathrm{OSR}{\cdot}\mathrm{F_s}$. For sequence A or B, the maximum transmission bandwidth is reduced to $\mathrm{IF}/(2{\cdot}\mathrm{OSR})$ due to the added zeros. Nevertheless, the high-frequency signal replica exists for both RZ patterns of $\{\mathrm{S},\ 0\}$ and $\{0,\ \mathrm{S}\}$. Therefore, sequence A and sequence B can be multiplexed in the time domain to double the data rate.

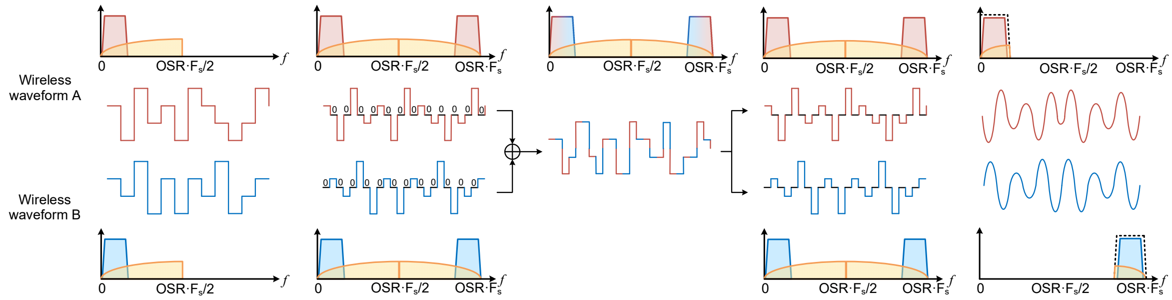

Fig. 1: Schematic diagram of IF-free RoF transmission based on low-pass delta-sigma modulator and RZ shaping. OSR: over-sampling rate; F_s: sampling rate of low-pass DSM.

At the receiver side, sequences A and B are first separated by de-multiplexing in the time domain. Afterwards, either a low-pass or high-pass filter is applicable to extract the signal at the desired band because both signal replicas convey the same information. It should be noted that a conjugation operation is needed for high-frequency band reception.

Experimental Setup

Fig.2(a) depicts the experimental setup and DSP stacks. At the transmitter side, the wireless waveform is emulated by QAM symbol mapping, up-sampling, and root-raised cosine (RRC) shaping with 0.01 roll-off. Then the waveform is over-sampled and fed into a low-pass DSM implemented on 4th-order cascaded resonator feedback (CRFB) structure. Here 1-bit, 1.5-bit, and 2-bit DSM correspond to 2-, 3-, and 4-level quantized optical signals. The noise transfer functions with different over-sampling rates are displayed in Fig.2(b), and the zeros and poles distribution of a 2-bit DSM with an over-sampling rate of 20 is plotted in Fig.2(c). Fig.2(d) shows the evolution of signal spectra. The high-frequency region is occupied by quantization noise after low-pass DSM, and signal replica around 28 GHz can be observed after RZ shaping. The DSM outputs are then interleaved and encapsulated with a 2048-symbol preamble for both frame synchronization and channel equalization. Due to the limited tuneable range of the arbitrary waveform generator (AWG, M8194), the signal is re-sampled and finally generated by the AWG operating at 112/120/96-GSa/s sampling rates for 2-/1.5-/1-bit DSM. Then we use a 40-GHz Mach-Zehnder modulator (MZM) biased at the quadrature point to modulate the electrical signal. The optical carrier comes from an external cavity laser (ECL) centered at 1550-nm wavelength. In our experiment, we employ a wave-shaper to conduct optical dispersion compensation. It can be replaced by vestigial sideband [15] or single sideband shaping [16] schemes considering the cost-sensitive feature in fronthaul.

After transmission over 10-km single-mode fiber (SMF), the received optical signal is first detected by a 50-GHz photodiode (PD) and then amplified by a 50-GHz electrical amplifier (EA). The electrical waveform is sampled and stored by a real-time oscilloscope (RTO) operating at 128-GSa/s. In the offline DSP, the captured waveform is re-sampled to 2 sample-per-symbol (SPS), synchronized and equalized by a $T_s/2$-spaced 3-order sparse Volterra equalizer with diagonal-terms only. The tap lengths are 81, 9, and 5 for the 1st, 2nd, and 3rd-order kernels, respectively. After symbol decision, the two sequences are separated and pass through a low- or high-pass filter to remove the out-of-band quantization noise. Finally, the SNR and EVM values are

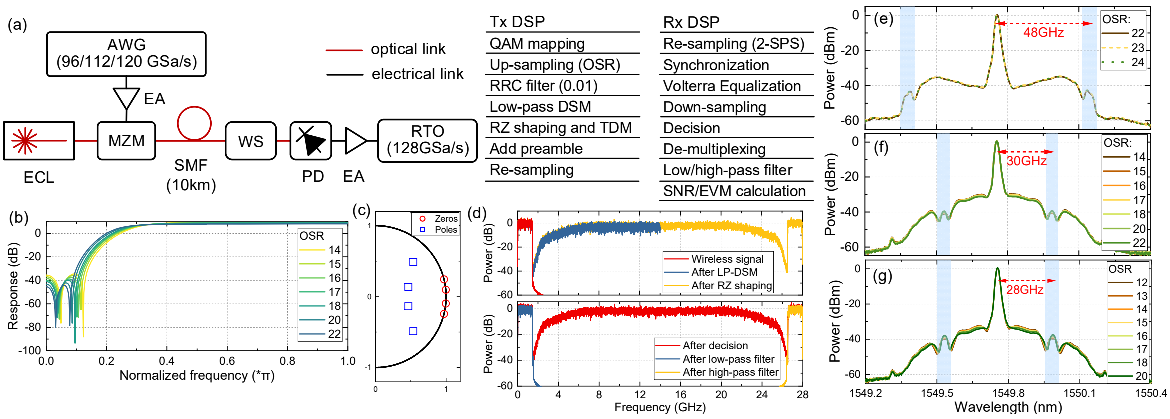

Fig. 2: (a) Experimental setup and DSP stacks. (b) Frequency response of noise transfer function of 2-bit low-pass DSM. (c) Zeros and pols of the noise transfer function using 2-bit DSM at OSR=20. (d) Signal spectra at different DSP stages. Measured optical spectra with (e) 1-bit DSM, (f) 1.5-bit DSM, and (g) 2-bit DSM.

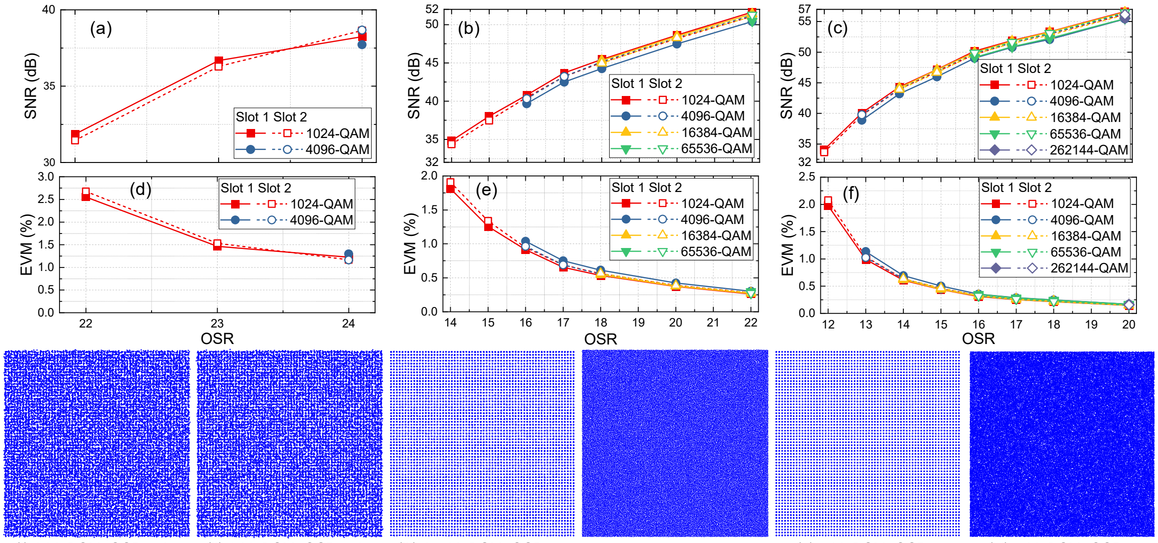

(i) 1-bit DSM, OSR=24 2^{12}-QAM (Slot 1) , 37.8dB
(ii) 1-bit DSM, OSR=24 2^{12}-QAM (Slot 2) , 38.6dB
(iii) 1.5-bit DSM, OSR=22 2^{12}-QAM (Slot 1) , 50.4dB
(iv) 1.5-bit DSM, OSR=22 2^{16}-QAM (Slot 1) , 50.4dB
(v) 2-bit DSM, OSR=20 2^{12}-QAM (Slot 1) , 55.4dB
(vi) 2-bit DSM, OSR=20 2^{18}-QAM (Slot 1) , 55.5dB

Fig. 3: (a)-(c) Measured SNR, and (d)-(f) EVM versus OSR with different modulation formats using 1-bit, 1.5-bit, and 2-bit DSM at 10km SMF. (i)-(vi) recovered constellations with 1-/1.5-/2-bit DSM after 10km transmission, respectively.

calculated based on the recovered constellations.

Fig.2(e)-2(g) present the optical spectra with 1-, 1.5-, and 2-bit DSM, respectively. The spacing between the optical carrier and signal are ~0.23 nm, 0.24 nm, and 0.38 nm, which is equivalent to 48 GHz, 30 GHz, and 28 GHz, respectively. The gradual decreasing of high-frequency component is caused by the modulator bandwidth limitation, which is compensated after channel equalization and decision at the receiver side.

Results and Discussions

Fig.3(a)-3(c) show the measured recovered SNR of wireless waveform versus over-sampling rate with 1-, 1.5-, and 2-bit DSM after 10-km SMF transmission, respectively. The solid and hollow points correspond to the sequences at time slot 1 and 2, which exhibit almost the same SNR values. It reveals that the RZ shaping and interleaving scheme can make up for the coding redundancy without penalty. We also compare the reception performance using a low- or high-pass filter for the same time slot. Two types of filters result in the same recovered SNR once the bandwidth limitation is compensated by the receiver-side DSP. For 1-, 1.5-, and 2-bit DSM, the recovered SNR are 38.1 dB, 50.8 dB, and 55.8 dB at OSR of 24, 22, and 20, which can support 4096-QAM, 65536-QAM, and 262144-QAM transmission, respectively. The SNR improvement can be attributed to the reduced quantization interval of the quantizer inside the DSM. More importantly, the recovered SNR rises with the over-sampling rate, making it possible to deliver an even higher-order modulation format with superior high fidelity.

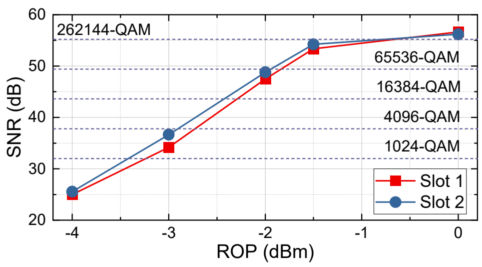

Fig. 4: Measured SNR versus ROP with 2-bit DSM at OSR of 20 after 10km SMF transmission.

Fig.4(a) shows the measured SNR versus received optical power (ROP) after 10km SMF transmission. 2-bit DSM is used with an over-sampling rate of 20. When the ROP is higher than -1.5 dBm, the recovered SNR decreases slightly thanks to the digital regeneration ability. Then the recovered SNR goes down rapidly as the electrical noise dominates the impairment. At the SNR thresholds, the measured ROP sensitivity are -3.4, -2.8, -2.4, -1.8, and 0.3 dBm for 1024-QAM to 262144-QAM, respectively.

Conclusions

To summarize, we propose and experimentally demonstrate a low-complexity IF-free RoF scheme based on low-pass DSM. Both Sub-6GHz and mmW band are supported thanks to the signal replicas after RZ shaping. The proposed scheme can support the maximum carrier frequency of $F_s/2$ and signal bandwidth of $F_s/(OSR)$. Based on a single wavelength and a single intensity modulator, we achieve 50.4Gb/s 262144-QAM, 43.6Gb/s 65536-QAM, and 48Gb/s 4096-QAM delivery at 28 GHz, 30 GHz, and 48 GHz carrier frequency, respectively. The results indicate a potential candidate for multi-band mobile fronthaul with high fidelity.

Acknowledgements National Key R&D Program of China (2022YFB2903500). National Natural Science Foundation of China. (62271305, 62001287).

References

[1] S. Chen, Y. C. Liang, S. Sun, S. Kang, W. Cheng, and M. Peng, "Vision, requirements, and technology trend of 6G: how to tackle the challenges of system coverage, capacity, user data-rate and movement speed," *IEEE Wireless Communications*, vol. 27, no. 2, pp. 218–228, 2020. DOI: 10.1109/MWC.001.1900333

[2] 3GPP TS 38.104, "5G NR: Base station (BS) radio transmission and reception (Release 15)," V15.3.0, Oct. 2018.

[3] X. Liu, H. Zeng, N. Chand, and F. Effenberger, "Efficient Mobile Fronthaul via DSP-Based Channel Aggregation," *Journal of Lightwave Technology*, vol. 34, no. 6, pp. 1556-1564, 2022. DOI: 10.1109/JLT.2021.3099726

[4] S. Ishimura, A. Bekkali, K. Tanaka, K. Nishimura, and M. Suzuki, "1.032-Tb/s CPRI-Equivalent Rate IF-Over-Fiber Transmission Using a Parallel IM/PM Transmitter for High-Capacity Mobile Fronthaul Links," *Journal of Lightwave Technology*, vol. 36, no. 8, pp. 1478-1484, 2018. DOI: 10.1109/JLT.2017.2787151

[5] X. Liu, "Enabling Optical Network Technologies for 5G and Beyond," *Journal of Lightwave Technology*, vol. 40, no. 2, pp. 358-367, 2016. DOI: 10.1109/JLT.2021.3102220

[6] H. Ji, C. Sun, and W. Shieh, "Spectral Efficiency Comparison Between Analog and Digital RoF for Mobile Fronthaul Transmission Link," *Journal of Lightwave Technology*, vol. 38, no. 20, pp. 5617-5623, 2020. DOI: 10.1109/JLT.2020.3003123

[7] D. Che, "Analog vs Digital Radio-Over-Fiber: A Spectral Efficiency Debate From the SNR Perspective," *Journal of Lightwave Technology*, vol. 39, no. 16, pp. 5325-5335, 2021. DOI: 10.1109/JLT.2021.3102220

[8] J. Wang, Z. Jia, L. A. Campos, and C. Knittle, "Delta-Sigma Modulation for Next Generation Fronthaul Interface," *Journal of Lightwave Technology*, vol. 37, no. 12, pp. 2838-2850, 2020. DOI: 10.1109/JLT.2018.2872057

[9] R. Schreier and G. C. Temes, "Understanding Delta-Sigma Data Converters," New York, NY, USA: Wiley, Nov. 2004.

[10] J. Wang, Z. Yu, K. Ying, J. Zhang, F. Lu, M. Xu, L. Cheng, X. Ma, and G.-K. Chang, "Digital Mobile Fronthaul Based on Delta–Sigma Modulation for 32 LTE Carrier Aggregation and FBMC Signals," *Journal of Optical Communications and Networking*, vol. 9, no. 2, pp. A233-A244, 2017. DOI: 10.1364/JOCN.9.00A233

[11] J. Wang, Z. Jia, L. A. Campos, L. Cheng, C. Knittle, and G.-K. Chang, "Delta-Sigma Digitization and Optical Coherent Transmission of DOCSIS 3.1 Signals in Hybrid Fiber Coax Networks," *Journal of Lightwave Technology*, vol. 36, no. 2, pp. 568-579, 2018. DOI: 10.1109/JLT.2017.2775858

[12] H. Li, et al., "Real-Time 100-GS/s Sigma-Delta Modulator for All-Digital Radio-over-Fiber Transmission," *Journal of Lightwave Technology*, vol. 38, no. 2, pp. 386–393, 2020. DOI: 10.1109/JLT.2019.2931549

[13] S. Jang, B. Park, and S. Hong, "Digital radio-over-fiber system with multi-pulse Manchester encoding-assisted delta-sigma modulation," Optics Express, vol. 25, no. 7, pp. 8335–8349, 2017. DOI: 10.1364/OE.25.008335

[14] Y. Zhu, Xiansong Fang, L. Yin, F. Zhang, and W. Hu, "Radio-over-Fiber Transmission Supporting 65536-QAM at 25GHz Band with High-Pass Delta-Sigma Modulation and RF fading Mitigation," in Proc. Optical Fiber Communication Conference (OFC), 2022, paper Tu2G.2. DOI: 10.1364/OFC.2022.Tu2G.2

[15] Y. Zhu, L. Li, X. Miao, and W. Hu, "Time skew enabled vestigial sideband modulation for dispersion-tolerant direct-detection transmission," *Optics Letters*, vol. 45, no. 22, pp. 6138–6141, 2020. DOI: 10.1364/OL.406146

[16] S. T. Le, K. Schuh, M. Chagnon, F. Buchali, and H. Buelow, "1.53-Tbps CPRI-Equivalent Data Rate Transmission with Kramers-Kronig Receiver for Mobile Fronthaul Links," in Proc. *European Conf. Optical Communication* (ECOC), 2018, paper We4B.4. DOI: 10.1109/ECOC.2018.8535539